

Chapter 2

Mercury and Venus: Significant Results from MESSENGER and Venus Express Missions

Sanjay S. Limaye

2.1 Introduction

Understanding how the solar system evolved has been one of the driving reasons for exploring the solar system until recently. Now the focus includes planets around other stars and particularly terrestrial planets and habitability. Mercury and Venus are two extreme members in our solar system but are poorly understood. Our closest planetary neighbors, with their proximity to the sun made it challenging to learn much about them from telescopes, as they are accessible for only a short time before sunrise or after sunset for large telescopes (due to scattered light and sensitive detectors). Venus with its global cloud cover made it impossible to learn about its surface, until new advances in radar and microwave techniques. Only partly surveyed by Mariner 10 from three fly-bys during 1974–1976, Mercury remained enigmatic until MESSENGER. By contrast, Venus has been explored from fly-by spacecraft, orbiters, entry probes and landers and even balloons, yet the major science questions have only become sharper. MESSENGER and Venus Express, the two current spacecraft visitors from Earth to the innermost, entered the final phase of their mission lives in summer 2014 as the fuel required for orbit maintenance was depleted. Orbiting Venus since 15 April 2006, Venus Express conducted an aerobraking experiment in June 2014. It collected its last observations on 27 November 2014 when the fuel was exhausted during orbit raise maneuvers, and the spacecraft entered the atmosphere on 18 January 2015. Over more than eight years of observing Venus from its 24 h, polar elliptic orbit, it collected a large amount of data from its operating instruments which have provided new insights into the atmosphere of Venus and to a limited extent, its surface. The MESSENGER spacecraft also observed Venus on its third fly-by of Venus which also yielded some new results.

S.S. Limaye (✉)
University of Wisconsin, Madison, USA
e-mail: sanjay.limaye@ssec.wisc.edu

Mercury, the primary target of the MESSENGER spacecraft since it entered into orbit around Mercury on 18 March, 2011 now awaits its next visitor, BepiColombo, a joint mission of the European Space Agency (ESA) and the Japan Aerospace Exploration Agency (JAXA) to be launched in July 2016. MESSENGER made three fly-bys of Mercury on 14 January 2008, 6 October 2008, and 29 September 2009 and has provided a deeper understanding of the planet which was explored previously by Mariner 10 in 1970s.

The larger goal behind exploring the two innermost planets is the same – how did the terrestrial planets evolve? The differences between the two innermost planets—Venus with its thick atmosphere and Mercury without any significant atmosphere—are starker than the differences between the two outer members – Earth and Mars. The impact histories of the four planets are different. It is believed that the presence of the Moon and impacts affected the spin states of Earth and Mars but the evolution of the spin states of Mercury and Venus are not well understood.

Basic orbital information about the two innermost planets have been known for a few long time, but their rotation rates were measured only in the 1960s with the advent of radar. Details of their spin state – polar wander, changes in rotation rate are not yet known. Whether or not the two planets had moons at some point is also a question that is being considered. Mercury's iron rich composition is a challenge to understand in the context of the other terrestrial planets (Asphaug and Reufer 2014). However, Venus' backward spin raises questions about its orbital evolution. The cloud-shrouded surface of Venus could be penetrated only by radar to measure the rotation rate, but precise recognition from optical telescopes of surface features on Mercury; despite being devoid of cloud cover had been hampered by its proximity to the Sun. Knowledge about Mercury before the observations from MESSENGER has been summarized by Solomon (2003) and about Venus by Taylor (2006).

While Mercury at first glance from Mariner 10 pictures resembles the Moon with its crater-filled surface, they are quite different, except for being comparable in size and devoid of significant atmospheres. Even from Mariner 10 images it was apparent that the volcanic plains on Mercury are brighter than those on the Moon, suggesting different composition and weathering, and the impact history surmised from crater size distribution is different for the two objects. The craters are both volcanic and impact, and both surfaces show the presence of lobate scarps that have been used to infer global contraction. Interpretation of topography from Mariner 10 images suggested that Mercury has contracted, and recent estimates imply even greater contraction. Recent Lunar Reconnaissance Orbiter (LRO) images also reveal a small contraction of the Moon – only about 0.1 km (Watters et al. 2010), compared to about 8 km for Mercury (Byrne et al. 2014), as inferred from MESSENGER images. Surface compositions are also different – despite being very dense with a massive iron core, Mercury has less iron and more sulfur on the surface as compared to the moon, which may explain differences in the appearance of the volcanic plains.

Mercury is smaller in equatorial diameter (3,397 km) than Mars (4,880 km), and both are smaller than Venus (6,052 km) and Earth 6,378 (km). Mercury and Venus

have the most eccentric and the most circular orbits around the Sun ($e = 0.2056$ and $e = 0.0068$ respectively), but also have the smallest inclination (0.0° and 2.6° respectively), whereas Earth and Mars have intermediate eccentricities and moderate inclinations. Thus, Mercury and Venus have small seasonal variations – on Mercury the insolation is modulated only by the changing distance from the Sun over its year, whereas Earth and Mars show significant insolation variation over their circuits around the Sun. The combination of the spin rate and the orbital period give Mercury the longest solar day – 175.94 Earth days, followed by Venus at 116.74, with Mars at only slightly longer than Earth at 1.029 Earth days. This results in the solar system's largest range of surface temperatures on Mercury, from about 100 K to 700 K. Due to its thick atmosphere, temperatures on Venus range from ~ 100 K in the upper atmosphere (inferred from SOIR experiment data on Venus Express; Mahieux et al. 2012) to ~ 750 K at the surface (VeGa 2 lander, Linkin et al. 1986).

The two smaller inner planets also have the lowest surface pressures – negligibly small on Mercury and about 6.8 mb on Mars, compared to 1025 mb on average on Earth at sea level, and about 93,000 mb on Venus at the mean radius. Compared to Mars, Venus has low topographic relief: about 80 % of the surface lies within ± 1 km of the mean surface (6051.78 km radius) and about 51 % within ± 0.5 km. Thus the surface temperature and pressure variations due to topography are small. The temperature decreases with altitude at approximately 8 K/km near the surface and may have superadiabatic lapse rates if the VeGa 2 temperature profile (Linkin et al. 1986) is representative of the global conditions, or at least adiabatic (Seiff 1987).

The high pressure and high temperature conditions in the lower atmosphere of Venus imply that the ideal gas law is not valid there (Staley 1970). Carbon dioxide (96.5 % atmospheric abundance) and nitrogen (3.5 %) are supercritical under these conditions; however it is not known how their mixture behaves. It is only recently that the supercritical gases are being investigated theoretically (Bolmatov et al. 2014), but more work is needed for mixtures. How the properties of gases and mixtures of gases change when they approach supercritical conditions is not very well known yet. While the belief was that they change slowly, computer simulations suggest that the change is abrupt and experimental validation is needed. At the same time, Venera probes did not appear to reveal any effect of the supercritical conditions, so some investigation is needed to verify the effect.

Venus has no internal measureable magnetic field, while Mars had an internal magnetic field in the past that disappeared some time ago, perhaps because its core solidified and the dynamo stopped. Mercury and Earth are known to have liquid outer cores, but whether Venus has a liquid outer core is not yet known. The absence of a liquid core is suggested only by the absence of a magnetic field, but the field could be absent if convection is suppressed. The case of the missing magnetic field of Venus is still a puzzle.

Both the Venus Express and MESSENGER missions had set science goals that led to their competitive selection for implementation. Those goals have been met, but the larger questions still await further analysis and interpretation with more observations to answer the new questions arising from the new results. A summary of the results from MESSENGER and Venus Express is presented below.

2.2 Mercury: Discoveries from MESSENGER

MESSENGER mission intended to answer the following six questions:

- Why is Mercury so dense?
- What is the geologic history of Mercury?
- What is the nature of Mercury's magnetic field?
- What is the structure of Mercury's core?
- What are the unusual materials at Mercury's poles?
- What volatiles are important at Mercury?

Major discoveries by MESSENGER include confirmation of a large iron core, presence of water ice and organic material in shadowed craters, presence of sulfur on the surface and an asymmetric magnetic field. Presence of ice was suspected from radar observations of the planet more than two decades ago that showed high reflectivity regions. MESSENGER observations from three different MESSENGER experiments confirmed the presence of water ice. The neutron experiments showed a hydrogen-rich layer in the bright radar locations, consistent with pure water ice. The laser altimeter carried by MESSENGER showed irregular dark and bright deposits in the craters near the north pole. The following subsections discuss these discoveries in further detail.

2.2.1 Surface

High spatial resolution imaging from narrow (monochrome) and wide angle (eleven narrow band filters) cameras of the MESSENGER Dual Imaging System (MDIS, Hawkins et al. 2007) has produced near global coverage of the Mercury. The MESSENGER Laser Altimeter (MLA, Cavanaugh et al. 2007) has yielded global elevation maps of the Northern hemisphere. Due to the eccentric orbit with periapsis latitude near the north pole, the range to the surface is too large for observations in the Southern hemisphere. These new datasets have revealed new insights into the processes modifying the planet's surface, including tectonics, volcanism, impact cratering, and volatile accumulation.

Prior to MESSENGER observations, the role of volcanism on Mercury was uncertain. The smooth plains within craters and between craters could be attributed to both eruptions and ejecta from impacts, as distinguishing features corresponding to each process were not discerned at the resolution of Mariner 10 images (Solomon 2003). Infrared (MASCS), gamma ray (GRNS) and X-ray (XRS) spectrometers also provide composition information key to understanding the surface evolution and the Laser Altimeter (MLA) has provided information about topographic relief.

Figure 2.1 shows a natural color global composite of many MDIS images. An enhanced view is shown in the bottom panel of this figure. The enhanced color was produced by using images from the color base map imaging campaign during

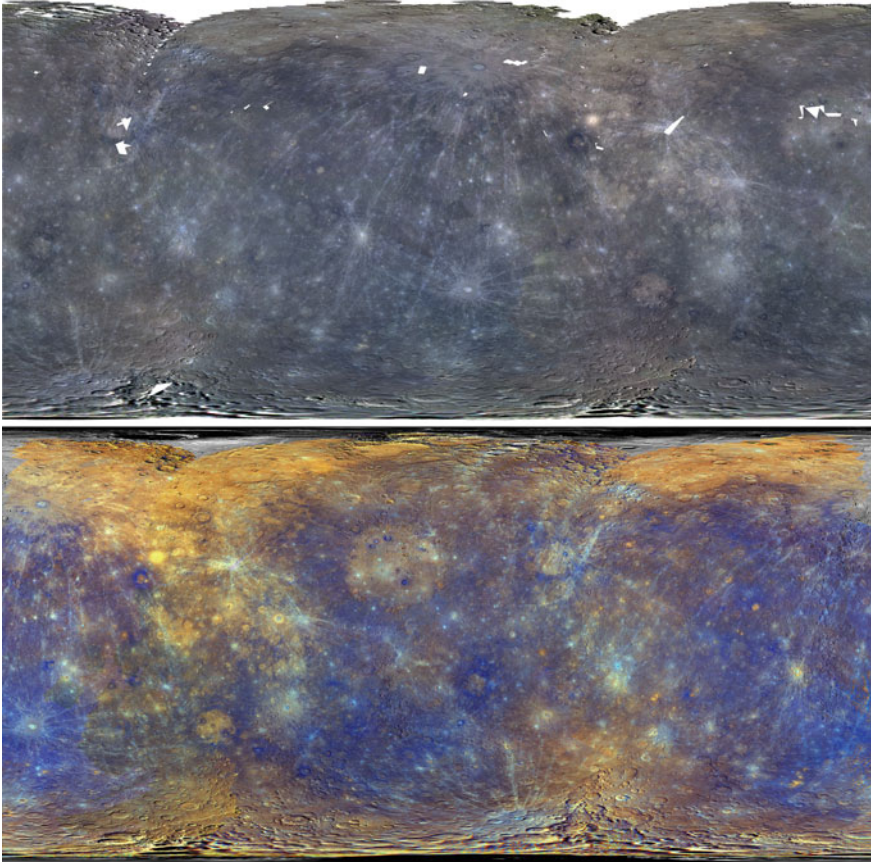


Fig. 2.1 The color global mosaic is comprised of 8 narrow-band color filters of the MDIS Wide Angle Camera (WAC), while the 3-color northern hemisphere mosaic provides higher resolution but only in 3 of the narrow-band filters. Both products below are the latest as of March 7, 2014 (top). Placing the 1000-nm, 750-nm, and 430-nm filters in the red, green, and blue channels, respectively, produced the enhanced-color mosaics available below (bottom). Credit: NASA/Johns Hopkins University Applied Physics Laboratory/Arizona State University/Carnegie Institution of Washington. http://messenger.jhuapl.edu/gallery/sciencePhotos/image.php?image_id=234

MESSENGER's primary mission. These colors are not what Mercury would look like to the human eye, but rather the colors highlight the chemical, mineralogical, and physical differences between the rocks that make up Mercury's surface. This specific color combination places the second principal component in the red channel, the first principal component in the green channel, and the ratio of the 430 nm/1000 nm filters in the blue channel. The color differences suggest compositional differences on the surface and that some of the material may have been exposed due to impact processes. The deposits due to impacts can be seen in all parts of the crater – rim, central peak and the (Ernst et al. 2010).

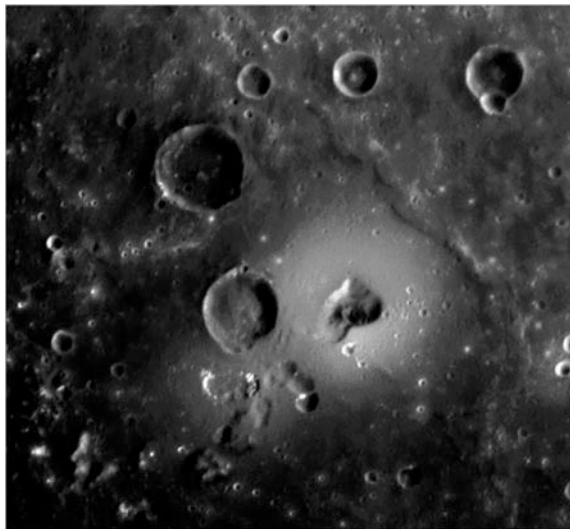
a. Volcanism and lava flows

Mariner 10 images of Mercury's surface showed the presence of smooth plains, but their volcanic origins were not unanimously accepted. Many scientists interpreted them to be due to fluidized ejecta from impacts (Byrne et al. 2013; Wilhelms 1976; Oberbeck et al. 1977), while others suggested otherwise based on embayment relations between the smooth plains, topography and estimates of ejecta from impacts (Murray et al. 1975; Strom et al. 1975; Robinson and Lucey 1997). One argument offered was based on studies of lunar volcanism: plains thought to be of volcanic origins from ground-based telescope images were later found to be due to impacts (Wilhelms 1976). During its first fly-by, MESSENGER images provided enough evidence to confirm the volcanic origins of the smooth plains. Subsequent fly-bys and orbital imaging data have now provided plenty of evidence of widespread surface volcanism and past large-scale lava flows extending over long distances. Unlike Venus, Mercury's volcanic features are not very diverse; generally smooth plains, while some interesting new details are being discovered from MESSENGER from the altimeter data and the images.

Figure 2.2 shows an example of a volcanic feature, possibly a shield volcano. Lava flows can be seen in many of the MESSENGER images (e.g., Fig. 2.3) and familiar features such as channel islands are also visible (Figs. 2.4 and 2.5). Eruptive or explosive volcanism is also evident in many parts (Fig. 2.6). Other surface features such as hollows are unique to Mercury (Fig. 2.7), as well as ridges and troughs (Fig. 2.8), which may have been altered or filled in by volcanic activity.

Images at high northern latitudes show lava flows with islands in the plains between craters as well as narrow, sinuous channels, similar to those seen on Venus, Mars, and the Moon (Leverington 2004) and consistent with formation by low viscosity lava flows (Byrne et al. 2013).

Fig. 2.2 The kidney-shaped depression is believed to be the volcanic vent of a shield-type volcano, similar to the volcanoes of Hawaii. The bright material around the vent is interpreted as material that fell after eruptions. *Photo credit: Science/AAAS*



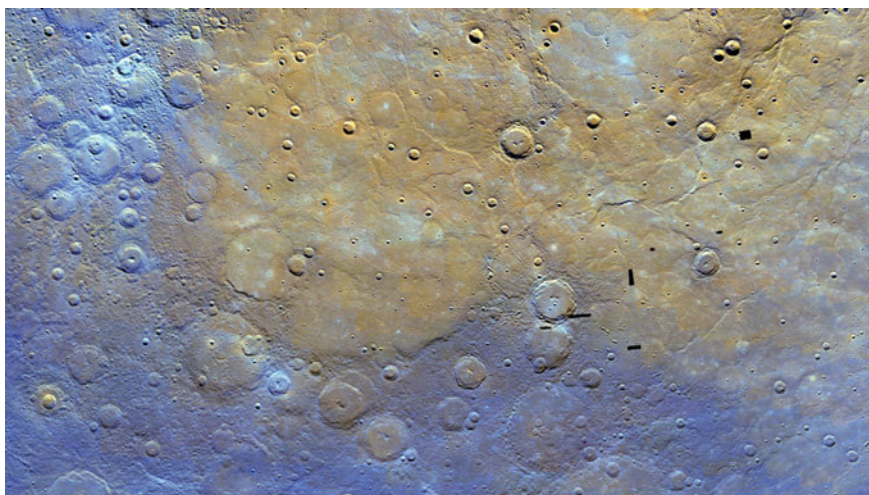


Fig. 2.3 Northern plains in enhanced color. The northern plains are seen here to be distinctive in color and thus composition from the surrounding terrain. The mosaicked images are shown with the 1000, 750, and 430 nm images in red, green, and blue, respectively. The scene is centered at 73 °N, 300 °E. Colors are based on a statistical method that highlights differences among the eight color filters, making variations in color and composition easier to discern. Credit: NASA/The Johns Hopkins University Applied Physics Laboratory/Carnegie Institution of Washington

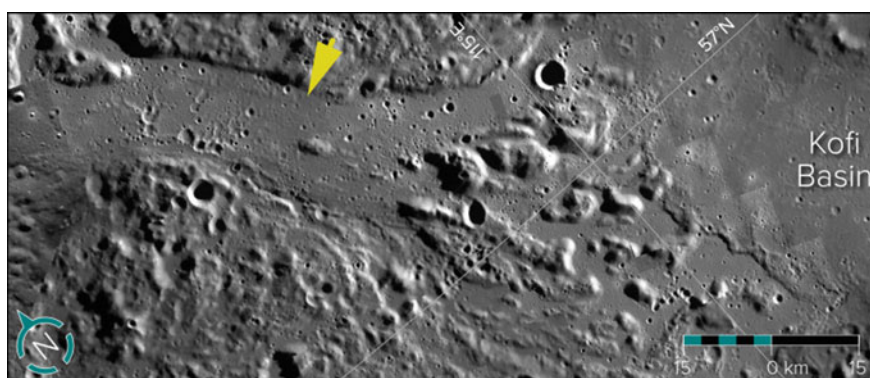


Fig. 2.4 Flat-floored channels near the northern smooth plains of Mercury (top), contain streamlined islands that appear to have been sculpted by hot lava as it flowed around them. A larger view of the islands is shown in the bottom image. Credit: NASA/JHU - APL/Carnegie Inst. of Washington

There are other differences also – on Mars the islands in the channel tend to be tear drop shaped which gives a clue to the flow direction. On Mercury the islands do not show such shapes, and the flow direction is not indicated by the shape but can be inferred from the laser altimeter data (Fig. 2.5). The source of the lava is also

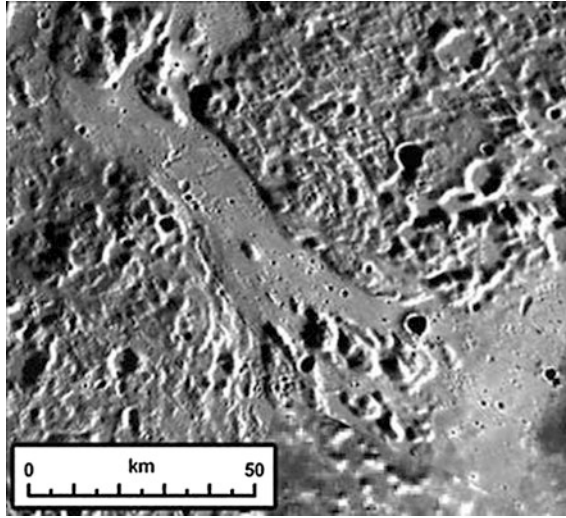


Fig. 2.5 A larger view of the islands is shown in the bottom image. Image Credit: NASA/JHU - APL/Carnegie Inst. of Washington

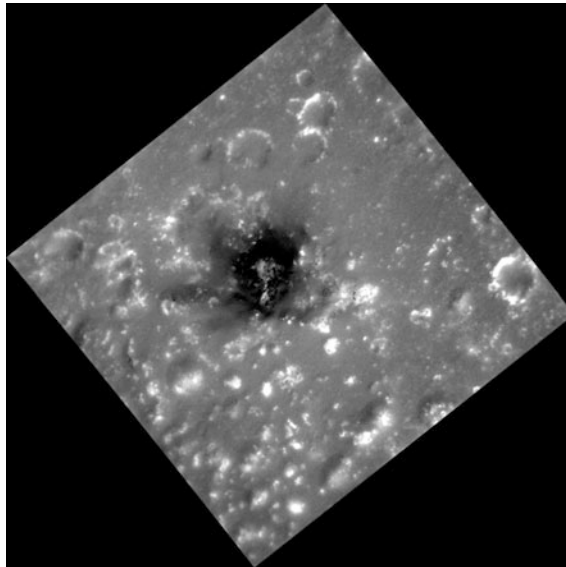


Fig. 2.6 This high-resolution image shows a region of the southern rim of the large Caloris basin. In the center is an irregularly shaped depression believed to be a pyroclastic volcanic vent. In this previously posted image, you can see this feature in the upper right as having a reddish color with a dark center. The composition of the dark material is not known. Most pyroclastic vents do not have this dark material, but other features do show small outcrops of it, such as Berkel and Seuss. Date acquired: May 05, 2013, Image Credit: NASA/Johns Hopkins University Applied Physics Laboratory

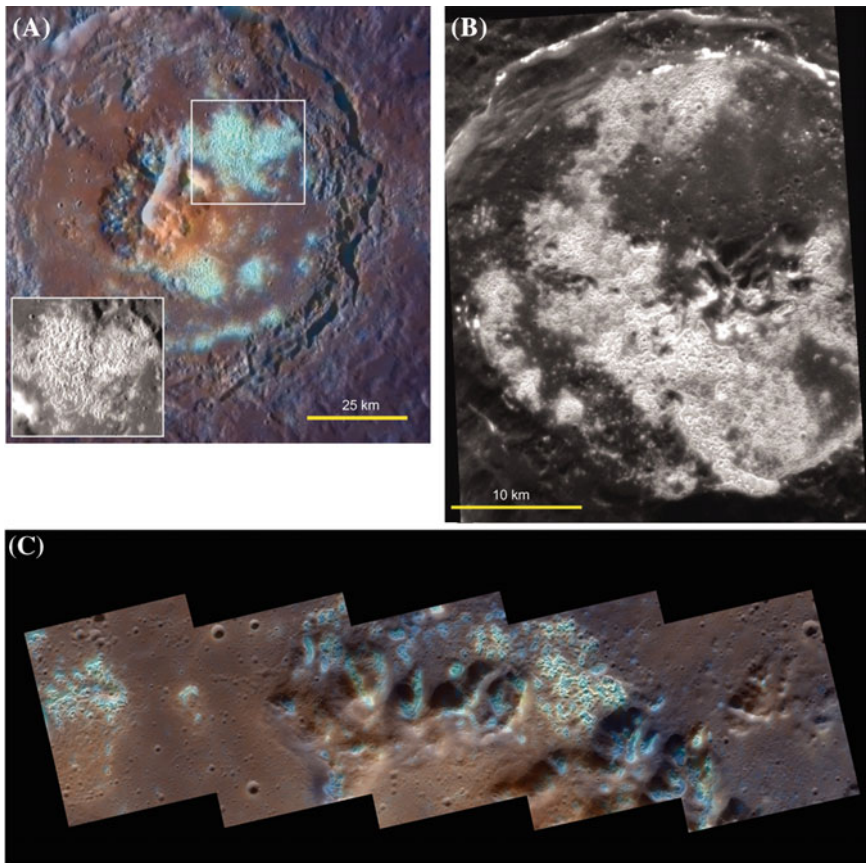


Fig. 2.7 (A) Tyagaraja crater, 97 km in diameter. Bright areas with blue color and etched texture correspond to a high density of hollows (inset). The central pit surrounded by reddish material is probably a pyroclastic vent. From monochrome image EN0212327089 M, 111 m/pixel, with enhanced color from the eight-filter set EW0217266882I (34). (B) Sander crater, 47 km in diameter. A high density of hollows occurs in the high-reflectance portions of the crater floor; others are found on the northern crater rim and wall terraces. Stereo analysis (35) indicates that any elevation differences between the high-reflectance and darker areas of the floor are ~ 20 m. Image EN0218289182 M, 30 m/pixel. (C). Hollows inside the Raditladi impact basin. Credit: NASA/Johns Hopkins University Applied Physics Laboratory/Carnegie Institution of Washington

not generally obvious. The other surprising indication is that the surface lava is not rich in Iron and Magnesium, but more sulfur rich, which is indicated by the color differences in the surface images.

b. Eruptive/Explosive Volcanism: Pyroclastic Deposits

The presence of pyroclasts implies presence of volatiles in the magma, its viscosity, ejection velocity and temperature, so the confirmation of such deposits first

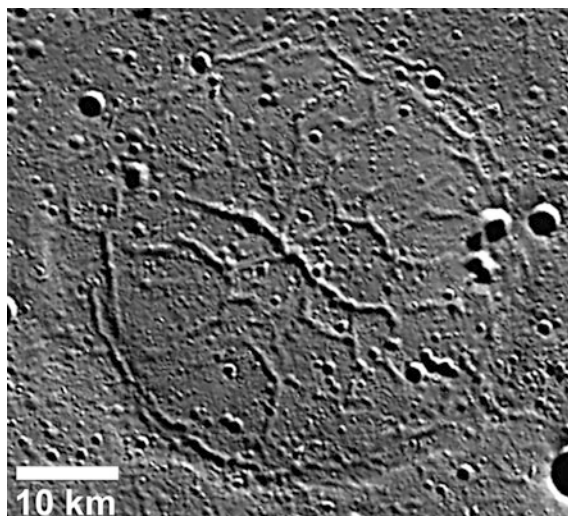


Fig. 2.8 This image shows large graben in a ghost crater on the floor of the Goethe impact basin on Mercury. The extensional troughs or graben are up to 2 km wide in this about 47-km-diameter ghost crater. Ridge and trough systems unique to Mercury have been observed in MESSENGER imagery. These features form in relation to “ghost craters,” impact craters that are filled and buried by volcanic deposits, but whose outline is revealed by ridges that form over the crater rim. Credit: NASA/APL

suspected from Mariner 10 images indicates that Mercury is not as depleted in volatiles as planetary formation theories had suggested. Further, the differences in color of such deposits and surrounding area from other regions of Mercury suggest compositional differences that provide clues about the volatiles and thermal history of the planet (Nittler et al. 2014; Kerber et al. 2011). Pyroclastic deposits detected from MESSENGER imaging data appear within impact craters (Fig. 2.5), suggesting that the eruptions occurred after the impacts as otherwise the impacts would have destroyed the deposits (Goudge et al. 2014). Fifty-one pyroclastic deposits have been identified from the near-global coverage of MESSENGER images from orbit after the initial tally from fly-by images (Kerber et al. 2009, 2011). Such features are also found on the Moon. However, after accounting for the different surface gravity, the distribution of deposit radius suggests that the eruption velocity on Mercury is likely much higher (Kerber et al. 2011).

The deposits are volatile-rich as determined from the multispectral images from the MESSENGER Dual Imaging System (MDIS) analyzed by Kerber et al. (2009, 2011). This detection is significant due to the indication of presence of volatiles on Mercury. Being so close to the Sun, it would appear that Mercury would be volatile-depleted (Wetherill 1994) as it is believed to have formed in the hot part of the solar nebula. Subsequent impacts and other heating events would have further

driven away the volatiles, and hence the detection of larger-than-expected deposits of volatiles will require a fresh look at the formation of the planet and its evolutionary history.

c. Hollows: Rimless Depressions

One of the strangest features discovered on Mercury are the occurrences in many parts of hollows or pits (Figs. 2.6 and 2.7). Hollows were found in the polar regions of Mars covered with carbon dioxide, but on Mercury these features are found on the rocky surface. High resolution images from MESSENGER revealed many irregular, shallow and rimless depressions for the first time (Blewett et al. 2011). Their age is relatively young as apparent from the fact that such hollows appear within impact craters, thus confirming that Mercury is not a static relic orbiting the Sun, but their origin is not entirely clear.

d. Ridges and Troughs

Some of the most unusual formations seen on Mercury are ridges and troughs, not seen on any other moon or planet. Mercury (Watters et al. 2012). Ridges are believed to be formed when impact craters are covered in volcanic ash deposits towards the rim, creating “ghost craters”. Troughs and ridges are believed to be formed due to extensional fault forming process and contraction resulting from cooling of the interior.

e. Impact Craters

Not all craters on Mercury are volcanic as can be expected. Figure 2.9 shows one of the high resolution images of the Cunningham impact crater. The central peak is seen in detail but the rays resulting from the falling debris are outside the image area.

f. Polar Ice Deposits

It was suggested decades ago (Watson et al. 1961) that permanently shadowed regions in polar craters on the moon may harbor water ice. In 1991, radar images of the polar regions of Mercury from Arecibo showed several radar bright regions (Slade et al. 1992) which were co-located with craters, and it was shown that water ice could survive for a long time on the surface of Mercury in shadowed regions (Vasavada et al. 1999). MESSENGER was equipped with instruments capable of detecting the presence of water ice and observations confirmed that water ice is indeed present in the permanently shadowed regions of polar craters. The laser altimeter observations recorded the presence of bright and darker deposits in the 1032 nm echoes from the shadowed regions from the poleward facing walls in the same locations as the radar echoes (Chabot et al. 2014). Paige et al. (2013) calculated the expected temperatures in the shadowed regions. The results show that the bright echoes (Fig. 2.10) are consistent with water ice and the darker regions with a coating of complex organic material on the ice, with impacts of comets and asteroids laden with organic compounds as the likely source (Lucey 2013).

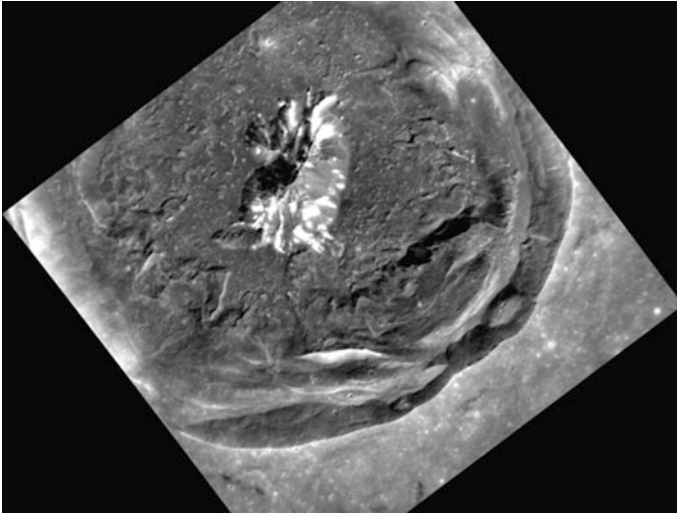


Fig. 2.9 This high-resolution view of Cunningham crater (~ 200 m/pixel) was recently acquired by MESSENGER. What cannot be seen in this image, which shows striking details of the crater's interior, is the extensive set of rays associated with Cunningham. The bright rays of Cunningham indicate that the crater is relatively young, having formed on Mercury likely within the last billion years. In this view, the preserved terraces of the crater walls, the well-defined central peak, and the limited number of overlying small craters are also all signs of Cunningham's relative youth

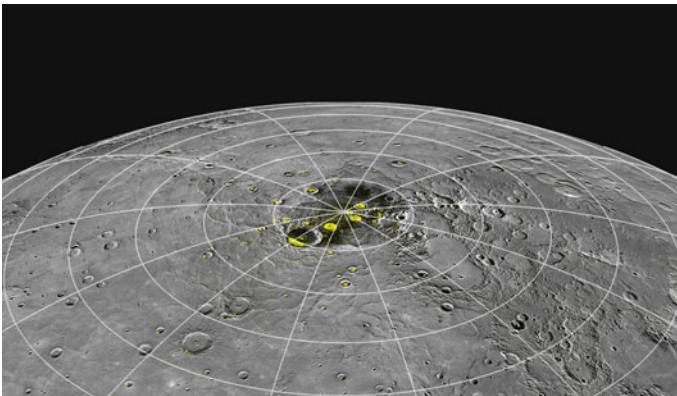


Fig. 2.10 Perspective view of Mercury's north polar region with the radar-bright regions shown in yellow. Credit: NASA/Johns Hopkins University Applied Physics Laboratory/Carnegie Institution of Washington

The composition of the polar deposits was confirmed indirectly from the detection of neutrons created when cosmic rays strike the planet (Lawrence et al. 2013). The inference is based on the process as follows. The neutrons travel

through the polar deposits and surface material, escaping into space where they are detected by the Neutron Spectrometer. The presence of hydrogen atoms within the ice in the polar deposits stop the neutrons from escaping into space, thus a drop in the rate of neutrons detected is believed to be due to the presence of hydrogen in the form of polar ice thus, a drop in the neutron detection rate can be related to the abundance of hydrogen and hence water ice in the polar deposits (Fig. 2.11).

Dark patches have also been observed in some of these deposits and are believed to be composed of organic compounds (Fig. 2.11). Figure 2.12 shows the calculated maximum temperatures reached in the northern polar regions of Mercury (Paige et al. 2013). The detailed thermal map of Mercury, and others that display additional thermal parameters, are the first to have been calculated from measurements of Mercury's topography by the MESSENGER MLA instrument. Mercury displays the most extreme range of surface temperatures of any body in the solar system. Regions that receive direct sunlight at the equator reach maximum temperatures of 700 K (800 °F), whereas regions in permanent shadow in high-latitude craters can drop below 50 K (−370 °F).

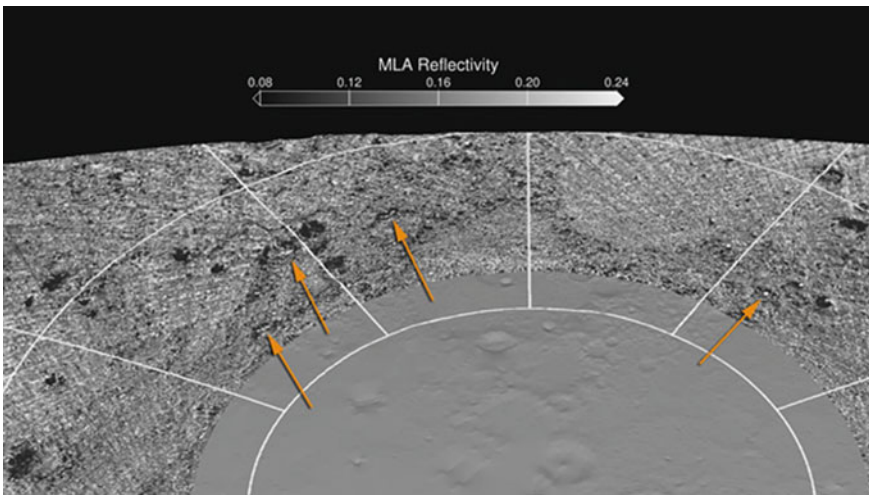


Fig. 2.11 Map of reflectivity determined from the Laser Altimeter data showing isolated areas of brighter and darker reflectance in areas of permanently shadow. Many of the brighter areas detected by MLA (as indicated by the arrows) are in unusually cold regions where surface water ice is predicted, as shown in Fig. 2.2. In some cases, the dark regions are somewhat larger than the areas predicted to have thermally stable water ice. *Credit: NASA/UCLA/Johns Hopkins University Applied Physics Laboratory/Carnegie Institution of Washington*

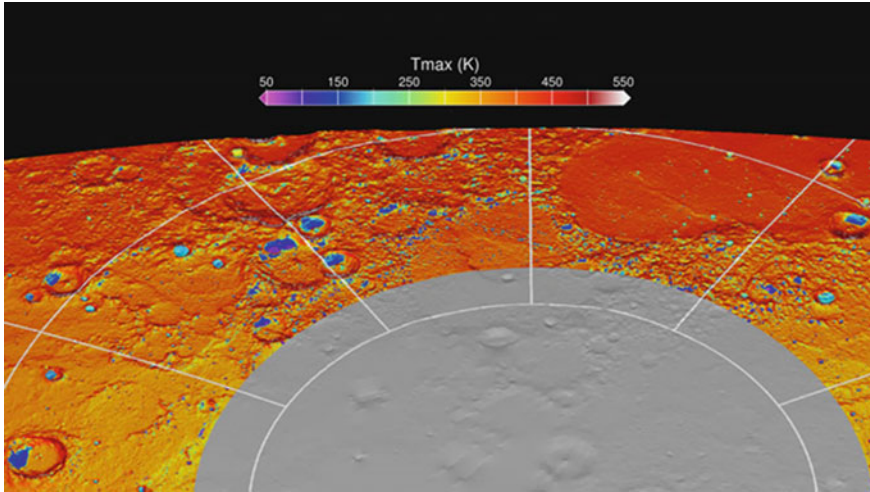


Fig. 2.12 Map of the maximum surface temperature reached over a two-year period over the north polar region of Mercury. In this view from above Mercury's north pole, there are numerous craters with poleward-facing slopes on which the annual maximum temperature is less than 100 K (-280°F). At these temperatures, water ice is thermally stable over billion-year timescales. Credit: David A. Paige, MESSENGER Participating Scientist, University of California, Los Angeles, California. Credit: NASA/UCLA/Johns Hopkins University Applied Physics Laboratory/Carnegie Institution of Washington

2.2.2 Mercury's Interior Structure and Gravity Field

a. Contraction of Mercury

Mercury is the only planet for which the contraction has been confirmed observationally. It is believed that all planets were very warm in their formative stages and have since cooled. With cooling, a decrease in size can be expected. Such global contraction due to cooling of the interior was first proposed as a mountain building process for Earth's surface, but the idea was criticized early (Dutton 1874). The solid planet, as it cools and shrinks, forms ridges and scarps, and by studying these formations from Mariner 10 coverage, it was inferred that the planet had shrunk in radius by an amount between 1 and 3 km, smaller than expected from predictions of Mercury's thermal history (Byrne et al. 2014). With global coverage from MESSENGER observations, a more comprehensive survey of ridges and scarps yields a higher value – about 5–10 km, more consistent with the thermal models. This is useful for understanding the history of the planet in terms of heat loss, tectonic and volcanic activity, and its metallic core.

b. Gravity Field and Internal Structure

Indications that Mercury has a molten core came from radar observations of the planet from Earth, prior to MESSENGER spacecraft's arrival at Mercury (Margot et al. 2007). By tracking the MESSENGER spacecraft accurately from the ground

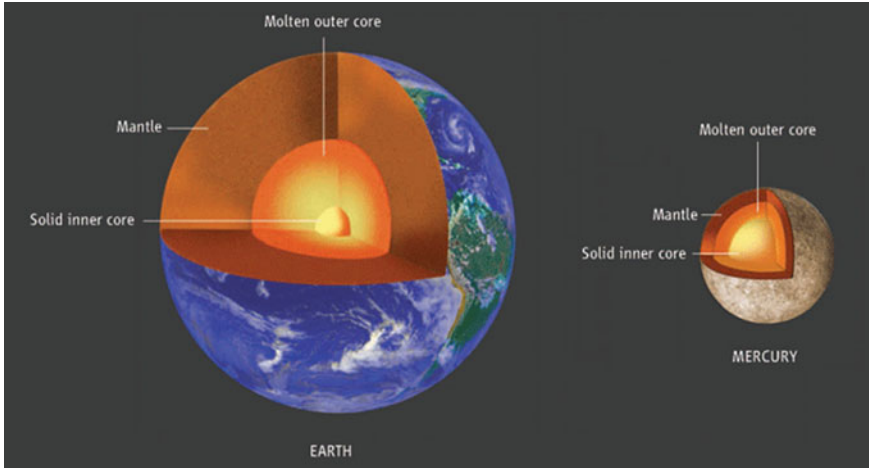


Fig. 2.13 The solid inner core and fluid outer core of Earth are shown to approximate scale. Mercury's outer core is now known to be fluid, but its radius and the nature and radius of any solid inner core remain to be determined. (Credit: NASA and The Johns Hopkins Applied Physics Laboratory)

stations, the northern hemisphere gravity field has been obtained, which reveals several mass concentrations. Another inference is that the low latitude crust is thicker than at higher latitudes. According to Margot et al. (2007), a model for Mercury's radial density distribution consistent with these results includes a solid silicate crust and mantle overlying a solid iron-sulfide layer, an iron-rich liquid outer core, and perhaps a solid inner core.

c. Interior

The discovery of a relatively weak magnetic field around Mercury by Mariner 10 led to the suggestion that the field was created by the dynamo effect from a molten core. Yet Mercury's small size should favor cooling and solidification of a liquid core. Thus the inference of a liquid core by monitoring the variations in the spin rate of the planet by bouncing radar signals was a surprise (Margot et al. 2007). These observations also pinned down the obliquity of Mercury to a high accuracy (2.11 ± 0.1 arc min) and found large amplitude librations in longitude (35.8 ± 2 arc s) which indicate that the core is at least partially molten and decoupled from the mantle (Fig. 2.13).

2.3 Exosphere of Mercury

Mercury's atmosphere was detected for the first time after hydrogen, helium, and atomic oxygen were detected on the dayside observations from ultraviolet spectrometer observations from Mariner 10. Presence of sodium, potassium, and calcium

was known before MESSENGER from ground based observations (Killeen et al. 2007) in the exosphere, and MESSENGER found magnesium. What characterizes Mercury's atmosphere, or more accurately exosphere (because of the low densities) is that the collisional processes are not with other atoms or molecules, but with the surface of the planet. Hydrogen and helium were believed to originate from the impinging solar wind, and other detected species arising from the interaction of the solar wind with the surface of Mercury through sputtering, photon induced desorption and vaporization. Thus the exosphere properties are affected by the orbital properties and also Mercury's magnetic field. The exosphere thus shows large variations in density with solar longitude and planet latitude. The polar regions which receive little incident sunlight act as cold traps for material that reaches the surface (Killen et al. 2007). Figure 2.14 shows a schematic view of the processes that play a role in maintaining the exosphere – (i) the incident sunlight stimulating desorption and thermal evaporation of volatiles from the surface (low energy process), (ii) sputtering (high energy process), and (iii) release of material from surface through meteoroid impact. The atoms can get ionized and interact with the magnetic field and the solar wind and radiation pressure while some, ejected with lower energies can fall back on the planet at a different location, some carried to the dark polar regions.

MESSENGER detected magnesium in the tenuous atmosphere for the first time, suggesting strongly that the metal is present in the crust since the atmosphere

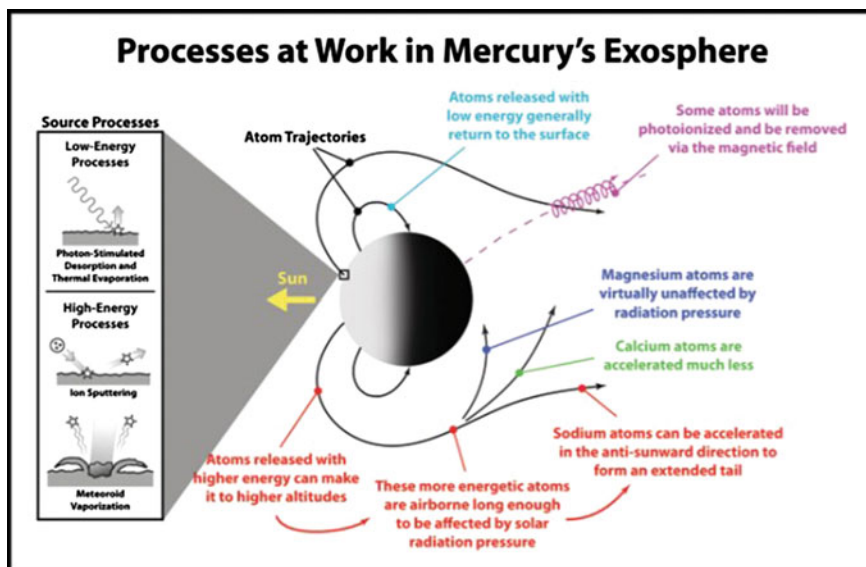


Fig. 2.14 Schematic illustration of the processes that generate and maintain Mercury's exosphere. Determining the relative importance of these processes through observations at different times and positions will yield insight into the interaction between Mercury's surface and the surrounding space environment

survives as atoms are ejected from the surface by the impacting solar wind, solar radiation and micrometeoroids. Prior observations had detected the presence of hydrogen, helium, sodium, calcium and potassium. One of the surprising discoveries from MESSENGER is a difference between the distributions of calcium and magnesium. Calcium abundance peaked near the equator, while magnesium was observed to be distributed more uniformly. Further, more calcium was detected near sunrise than at sunset, but not in sodium or magnesium amounts. Figure 2.15 shows the sodium atmosphere (“tail”) seen from MESSENGER during the second and the third fly-bys and results of modeling of the processes involved that determine the abundance. As in previous flybys, the distinct north and south enhancements in the emission that result from material being sputtered from the surface at high latitudes on the dayside are seen.

The mission has succeeded in obtaining valuable observations to address them. A fuller understanding will follow when the implications of the observations and the new questions raised are considered, and after new data from the BepiColombo mission.

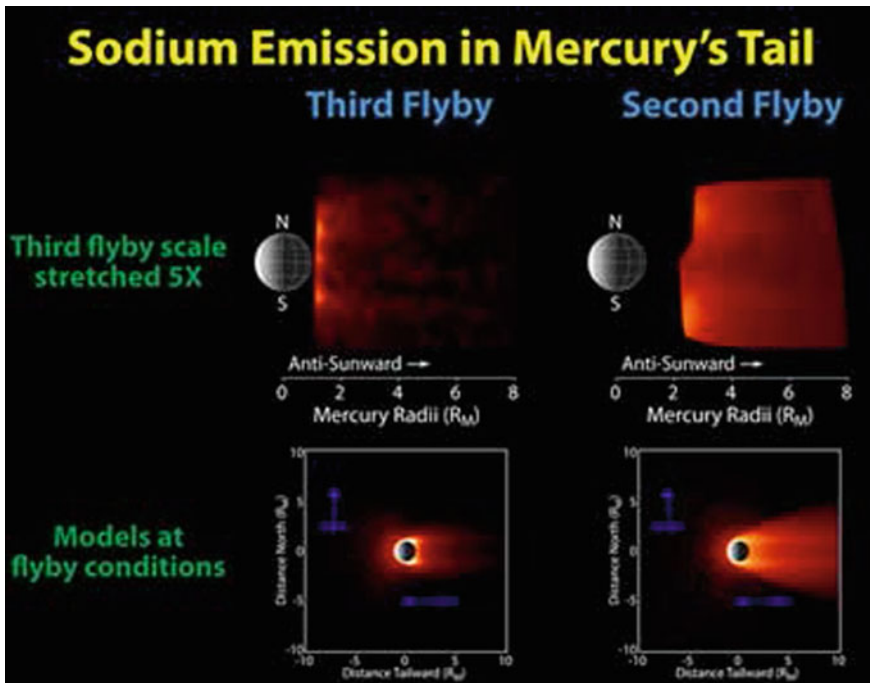


Fig. 2.15 Comparison of the neutral sodium observed during the second and third Mercury flybys to models. The top left and right panels show the same images as in Image 2.2, but the color scale for the third flyby has been stretched to show the distribution of sodium more clearly. The lower two panels show Monte Carlo models of the sodium abundance in Mercury’s exosphere for conditions similar to those during the two flybys. Credit: http://www.nasa.gov/mission_pages/messenger/media/flyby20091029.html

2.4 Venus: Results from Venus Express

Operating with most instruments initially designed for Mars, ESA's Venus Express has made many significant discoveries about Venus – its exosphere, atmosphere and surface. Its objectives were to study (Svedhem et al. 2009):

- Atmospheric structure
- Atmospheric dynamics,
- Atmospheric composition and chemistry
- Cloud layer and hazes
- Energy balance and greenhouse effect,
- Plasma environment and escape processes, and
- Surface properties and geology.

The mission formally ended on 18 January 2015 after making many discoveries. Among the most interesting discoveries made by Venus Express, the possible change in the rotation rate of Venus is perhaps most significant, followed by long term changes in the abundance of sulfur dioxide gas above the clouds, the presence of electrical activity, and the presence of a relatively narrow layer of increasing temperature in the exosphere, similar to Earth's stratosphere. Also significant are the detection of hydroxyl molecules escaping Venus, and detection of trace species such as ozone, isotopologues and temporal and spatial changes in the amounts of sulfur dioxide above the clouds, and carbon monoxide. Some of the significant discoveries from Venus Express are summarized below.

2.4.1 Atmospheric Circulation

One of the early discoveries from Venus Express from the insertion orbit was a spectacular view of the hemispheric vortex over the southern pole from VIRTIS. Imaging in near infrared (night side) and in reflected sunlight (dayside) from high above the southern pole, the single image captured the vortex and the dipole structure of its inner core, also seen in Pioneer Venus OIR observations (Taylor et al. 1980). Previously Suomi and Limaye (1978) argued that the hemispheric vortex on Venus was dynamically similar to a tropical cyclone. Limaye et al. (2009) showed that the dipole feature could be simulated numerically from a cyclone circulation model and the result of a dynamical instability. The vortex was also investigated from VIRTIS (Garate-Lopez et al. 2013; Luz et al. 2011) who also obtained the latitudinal profile of the zonal and meridional components of cloud features at latitudes near the pole. The structure of motion of the vortex in the infrared observations was also seen to be asymmetric about the pole (Fig. 2.16).

Long-term changes in the measured cloud motions measured from the Venus Monitoring Camera were reported by Khatuntsev et al. (2013) and also by Kouyama et al. (2013). Periodicities ranging from 4.1 to 5.0 days were found in the

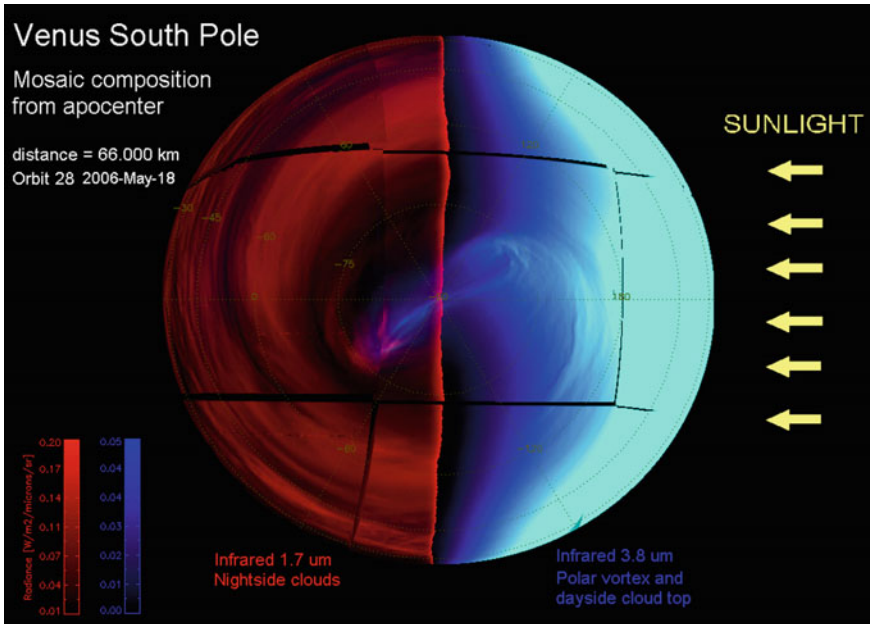


Fig. 2.16 A composite view of the day and night side of Venus from the VIRTIS instrument on Venus Express (ESA Image SEM49273R8F). This global view of Venus is a mosaic of several images taken by the Visible and Infrared Thermal Imaging Spectrometer (VIRTIS) on board ESA's Venus Express on 18 May 2007, at a distance of about 66 000 km from the planet. The images were obtained at 1.7 μ (left) and 3.8 μ (right) wavelengths. The wavelength used to obtain the left-hemisphere composite (1.7 μ) provides a dramatic global view of the night-side clouds in the lower atmosphere (approximately 45 km); while the wavelength used to obtain the right-hemisphere composite (3.8 μ) provides a view of the day-side cloud top

average cloud motions over during 2006–2012 resulting in an average value of 4.83 days. The long-term (Venus Express) average profile of zonal speed is comparable to the older, Mariner 10 results (Limaye and Suomi 1981) obtained from the short-term coverage of the fly-by observations, and both show the presence of a mid-latitude jet. The presence of such a jet is consistent with the hemispheric vortex. The Pioneer Venus average zonal flow did not show such a jet, but those results suffered from low image resolution and much longer time intervals between images (Limaye 2007). Further, these results are representative of the day-side as no nightside measurements are possible at the same vertical level from available data. The mean meridional flow over the Venus Express observations is also similar to Mariner 10, Pioneer and Galileo results – a weak poleward flow, peaking at about the same latitude (Fig. 2.17).

Over the duration of Venus Express observations, the average day-side cloud motions at low latitudes show a gradual increase in speed over time, but its validity remains uncertain. The chief reason may be due to the variable cloud morphology captured in the VMC images. The ability to measure cloud motions reliably

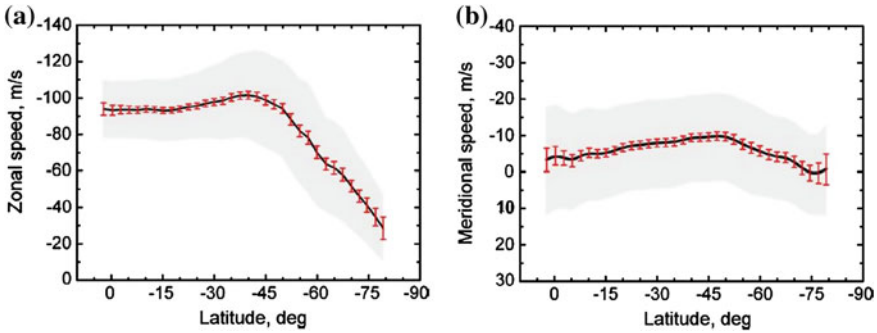


Fig. 2.17 Results from Khatuntsev et al. (2013) of average zonal (East-West) flow inferred from movements of clouds seen in images taken through the ultraviolet filter (365 nm) of the Venus Monitoring Camera (a) and North-South component (b). The negative sign for the zonal component implies flow from East to West (morning to evening direction) and poleward flow in the southern hemisphere. The shaded region indicates the standard deviation in one degree latitude bins. Some of the variability is due to the long-term changes in the measured cloud motions which is apparent in Fig. 2.18

depends on the visibility of discrete cloud features, and the morphology often makes it very difficult to find discrete features over the planet in the sun-lit portions of the planet, as the amount of haze that suppresses image cloud contrast increases towards the morning and evening terminators. Further, there is preliminary evidence that the representative cloud level that the measured motions correspond to may be variable over time by as much as ~ 1 km or more. Analysis of thermal structure data (Piccialli et al. 2012) and VIRTIS observations (Garate-Lopez et al. 2013) show that the vertical shear can be significant near the cloud top level, so the apparent trend in the temporal evolution may not be real (Fig. 2.18).

2.4.2 Rotation Rate of Venus – Length of Day Variations

By exploiting the fact that the temperature near the surface of Venus decreases with altitude, the Visible InfraRed Imaging Spectrometer (VIRTIS) on board Venus Express is able to relate the observed brightness temperature corresponding to the emitted radiation to topography. It was discovered that the rotation rate of Venus may be variable (Mueller et al. 2012) as the measured locations of some topographic features were different from expected values. The topography of Venus was obtained by the Magellan mission (Ford and Pettengill 1992). Mueller et al. (2012) discovered that the topographic features seen in the VIRTIS data are displaced somewhat from their corresponding topographic locations on Venus in the Magellan SAR data, which could result from a different orientation model, systematic offsets or a change in the rotation rate. Ground based radar estimates of the spin rate from data obtained during 2006–2009 are consistent (Schubert 2010) with

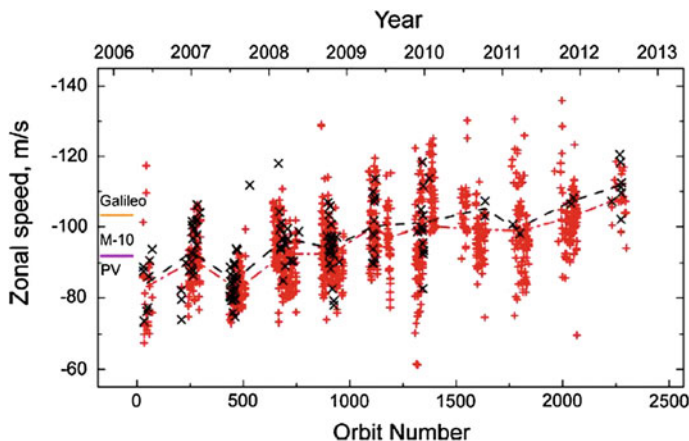


Fig. 2.18 Variations of the mean zonal wind speed at $20^\circ \pm 2.5^\circ \text{S}$ over the mission time. Symbols show orbital averages derived by manual (“x” and black dashed line) and digital (“+” and red dotted line) methods. The results from the Mariner 10 (92 m/s), Pioneer Venus (91.8 ± 3 m/s) and Galileo (103 m/s) missions for the same latitude zone are presented at the left edge of the plot for comparison. (For interpretation of the references to color in this figure legend, the reader is referred to Khatuntsev et al. 2013)

the 243.023 Earth days rotation rate estimated from VIRTIS data. It is also possible that Venus may exhibit measuring wobble arising out of planet’s interior structure. A change or a modulation in the rotation rate may also be expected through the exchange of angular momentum between the atmosphere and the solid planet (Schubert 1983).

2.4.3 Upper Atmosphere

2.4.3.1 Detection of Ozone in the Atmosphere of Venus

Although the same photochemistry is possible on Venus and Earth, the composition of the respective atmospheres leads to different processes. The lack of a large stratosphere with increasing temperature was an early clue to the lack of an ozone-rich layer on Venus. Nevertheless, the discovery of ozone on the night side in a 5–10 km thick layer between 90–120 km above the mean surface from the SPICAV instrument on Venus Express came as a surprise (Montmessin et al. 2011).

Ozone is believed to form by the release of an oxygen atom from photo-dissociation of carbon dioxide, combining with an oxygen molecule. Molecular oxygen is formed on the night side resulting from recombination of oxygen atoms transported from the day-side, as evidenced by the airglow (Gerard et al. 2008; Migliorini et al. 2011; Soret et al. 2014). The amount of ozone is ~ 1000 times

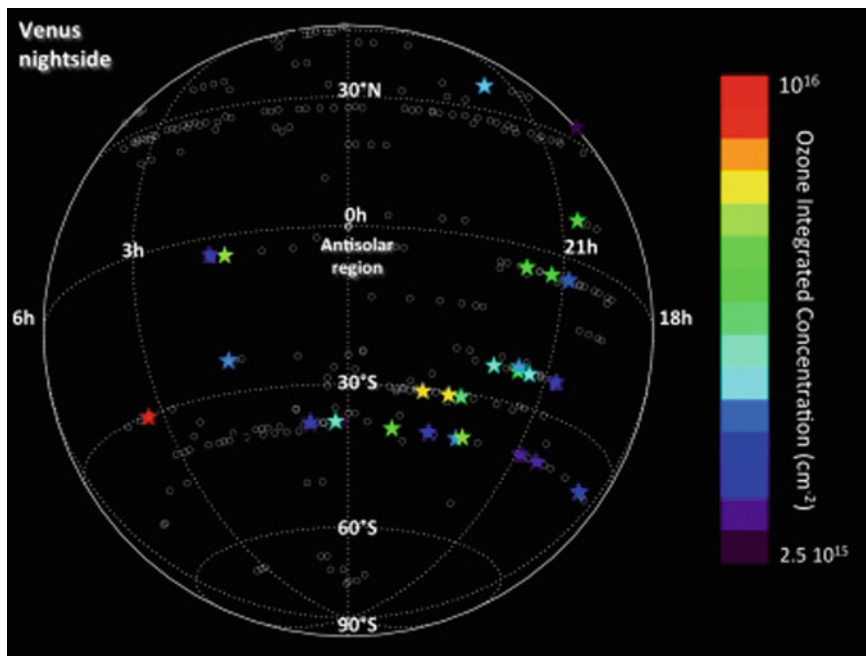


Fig. 2.19 SPICAV measurements of ozone in Venus atmosphere on the night side between 90–120 km altitude. Little ozone is detected at the midnight location at equator, a surprise

less than found in the stratosphere on Earth between about 9–15 km altitude (but ambient pressures are comparable for the ozone layer on Earth and Venus). It is not yet known whether ozone is catalytically destroyed near terminator by the same process that occurs in the polar stratospheric clouds on Earth. SPICAV observations do not provide good spatial coverage as they rely on stellar occultation, so more uniform coverage is needed to reveal the global pattern of ozone abundance in the atmosphere of Venus (Fig. 2.19).

2.4.3.2 Upper Atmosphere Cold Layer and Temperature Inversion

While it has been known for some time that the highest atmospheric temperature observed on any planet in our solar system is found on Venus near the surface, the detection of the coldest atmospheric temperature, about 100 K, also on Venus near the 125 km level, was a new discovery (Fig. 2.20).

Inferred from data collected by the Solar Occultation Infrared Radiometer instrument near the terminator in polar latitudes on Venus, the coldest layer may suggest the presence of frozen carbon dioxide particles (Mahieux et al. 2012). The atmospheric range of temperatures on Venus, from ~100 K to 750 K is comparable to the day-night difference in surface temperatures on the atmosphereless Mercury.

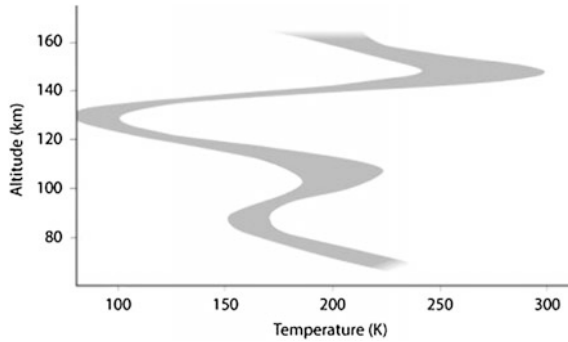


Fig. 2.20 The temperature profile along the terminator for altitudes of 70–160 km above the surface of Venus. The values were derived from the volume density of carbon dioxide molecules measured during solar occultation experiments by Venus Express’ SOIR instrument. The shaded curve shows the average range of values calculated from 59 measurements taken along the terminator from 88 °N to 77 °S, during different orbits between 2006 and 2011

But the other surprising features are two layers of increasing temperature with altitude – between about 90–100 km and between 130–150 km. The reason for the warm layer is not yet known.

2.4.4 Possible Recent Volcanism?

The extent of current volcanism is still unknown, but several different clues keep coming. One of the more compelling clues is a rise and decay in the abundance of sulfur dioxide measured above the cloud tops from SOIR/SPICAV experiment (Marcq et al. 2013). While a near-exponential decrease was measured from Pioneer Venus ultraviolet spectrometer (Esposito et al. 1988), a rise from the low levels was observed for the first time from Venus Express observations, peaking in 2007 and decreasing again. Esposito (1984) had proposed explosive volcanism injected large amounts of sulfur dioxide gas punching through the thick cloud layer, and a similar situation is suggested by the Venus Express observations. Dynamical transport by the global atmospheric circulation has also been suggested, but it is not understood how the circulation would lead to the observed rise and decay. One difficulty with both the Venus Express and the older Pioneer Venus observations is the lack of global coverage. Thus, it is plausible that the observed rise and fall is not globally representative, which does not negate the argument for episodic volcanism.

The rise and fall of sulfur dioxide in the upper atmosphere of Venus over the last 40 years, expressed in units of parts per billion by volume (ppbv) is shown in Fig. 2.21. The dataset on the left is mostly from NASA’s Pioneer Venus orbiter data (Esposito et al. 1988), which orbited Venus from 1978 to 1992. The dataset on the right shows results from the SOIR instrument observation at morning at evening terminators after Venus Express entered into orbit in 2006. A clear rise in the

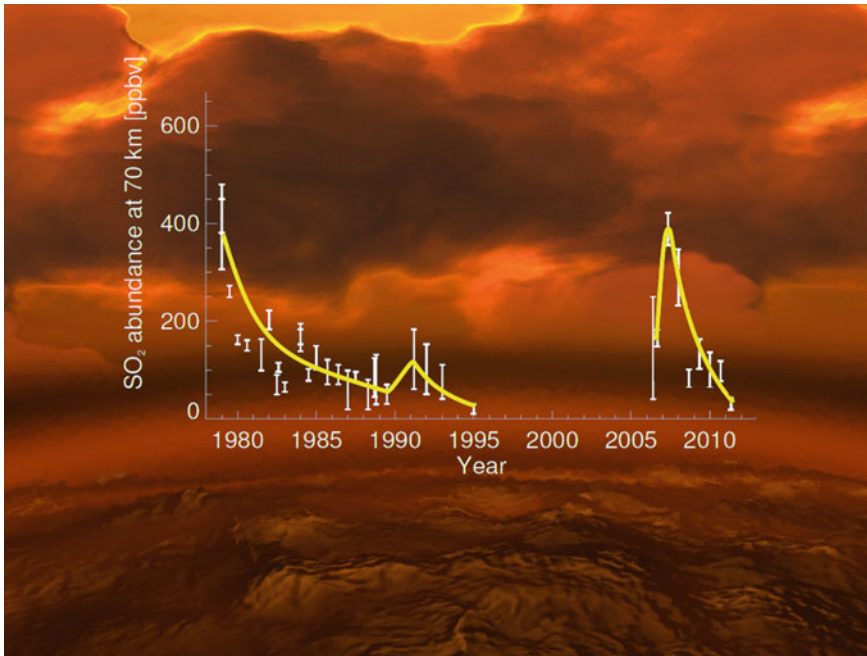


Fig. 2.21 A clear rise in the concentration of sulfur dioxide (SO_2) concentration was observed at the start of the mission, with a subsequent decrease. The increase in sulfur dioxide can be interpreted either as evidence for volcanic activity or for decadal-scale variations in the circulation of Venus' vast atmosphere. The data are superimposed on an artist impression of Venus, depicting a volcanic terrain surrounded by a thick, noxious atmosphere. Credit: ESA graphics (<http://sci.esa.int/venus-express/51187-rise-and-fall-of-sulphur-dioxide/>)

concentration of sulfur dioxide (SO_2) concentration was observed at the start of the mission, with a subsequent decrease.

Bondarenko et al. (2010) detected excess microwave emissions in 1993 in the Magellan radiometry data and concluded that this implied increased sub-surface temperatures due to emplacement of magma. Smrekar et al. (2010) also reported high emissivity locations coinciding with some potential hotspots in low latitude regions of Venus. An emplacement age of <2.5 Ma was argued based on the inference of limited surface weathering. Increased, transient high surface temperatures have also been inferred in some Venus Monitoring Camera near infrared images (Shalygin et al. 2014; Bazilevskiy et al. 2014).

While doubts can be raised about the validity of such claims of near-surface geologic activity due to and observational constraints and data processing issues, the diversity of different clues is intriguing. Current volcanism may explain many aspects of the dynamical behavior of the Venus atmosphere and confirm some of the assumptions about Venus. Nevertheless, a strong confirmation of an active current or recent volcanic eruption that would remove any doubts and remains a future observational prize.

2.5 Summary

MESSENGER and Venus Express missions have exceeded expectations about new knowledge gained about Mercury and Venus. Due to the orbital constraints posed by the elliptic orbit, MESSENGER data have poorer coverage or resolution in the southern hemisphere. At the end of the nominal mission the orbit was trimmed from a twelve hour period to one with an eight hour one, improving imaging ground resolution and also increasing coverage from the laser altimeter. In the near future, ESA/JAXA's BepiColombo mission will add significantly to the knowledge about Mercury.

JAXA's Akatsuki mission is expected to enter into Venus orbit during its second attempt in late November/early December 2015. Designed as a climate observing mission (Venus Climate Orbiter), it carries mostly cameras capable of taking pictures from ultraviolet to the thermal infrared wavelengths. The spacecraft is expected to be placed in a 7–10 day near equatorial orbit. The observations will perform a systematic investigation of the superrotation of the atmosphere. Many questions about Venus will remain unaddressed after this mission and the scientific community is eagerly awaiting a more comprehensive investigation of the planet regarding its surface, atmosphere and magnetosphere.

Acknowledgments I thank Ms. Rosalyn Pertzborn for editing the manuscript. This work was supported partially by NASA Grant NNX09AE85G, and by Space Science and Engineering Center, University of Wisconsin, Madison. Comments by two anonymous referees and Dr. A.B.S. Limaye were useful in improving the manuscript.

References

- Asphaug E, Reufer A (2014) Mercury and other iron-rich planetary bodies as relics of inefficient accretion. *Nat Geosci.* doi:[10.1038/ngeo2189](https://doi.org/10.1038/ngeo2189)
- Bazilevskiy A, Ignatiev N, Markiewicz W, Head J, Titov D, Shalygin EV (2014) Volcanism of Venus: insights from the VMC data analysis. In: 40th COSPAR scientific assembly. Held 2–10 August 2014, in Moscow, Russia, Abstract B0.7-1-14
- Blewett DT, Chabot NL, Denevi BW, Ernst CM, Head JW, Izenberg NR, Murchie SL, Solomon SC, Nittler LR, McCoy TJ, Xiao Z, Baker DMH, Fassett CI, Braden SE, Oberst J, Scholten F, Preusker F, Hurwitz DM (2011) Hollows on Mercury: MESSENGER evidence for geologically recent volatile-related activity. *Science* 333(6051):1856–1859. doi:[10.1126/science.1211681](https://doi.org/10.1126/science.1211681)
- Bolmatov D, Zav'yalov D, Gao M, Zhernenkov M (2014) Structural evolution of supercritical CO₂ across the Frenkel line. *Bo. J Phys Chem Lett* 5(16):2785–2790. doi:[10.1021/jz5012127](https://doi.org/10.1021/jz5012127)
- Bondarenko NV, Head JW, Ivanov MA (2010) Present-day volcanism on Venus: evidence from microwave radiometry. *Geophys Res Lett* 37:L23202. doi:[10.1029/2010GL045233](https://doi.org/10.1029/2010GL045233)
- Byrne PK, Klimczak C, Williams DA, Hurwitz DM, Solomon SC, Head JW, Preusker F, Oberst J (2013) An assemblage of lava flow features on Mercury. *J Geophys Res.* doi:[10.1002/jgre.20052](https://doi.org/10.1002/jgre.20052)
- Byrne PK, Klimczak C, Şengör AMC, Solomon SC, Watters TR, SA Hauck II (2014) Mercury's global contraction much greater than earlier estimates. *Nat Geosci* 7:301–307 doi:[10.1038/ngeo2097](https://doi.org/10.1038/ngeo2097)

- Cavanaugh JF, Smith JC, Sun XI, Bartels AE, Ramos-Izquierdo L, Krebs DJ, McGarry JF, Trunzo R, Novo-Gradac AM, Britt JL, Karsh J, Katz RB, Lukemire AT, Szymkiewicz R, Berry DL, Swinski JP, Neumann GA, Zuber MT, Smith DE (2007) The Mercury laser altimeter instrument for the MESSENGER mission. *Space Sci Rev* 131(1):451–479. doi:[10.1007/s11214-007-9273-4](https://doi.org/10.1007/s11214-007-9273-4)
- Chabot et al. (2014) Images of surface volatiles in Mercury's polar craters acquired by the MESSENGER spacecraft. *Geology* 42(10)
- Dutton CE (1874) A criticism of the contractional hypothesis. *Am J Sci* 8:113–123
- Ernst CM, Murchie SL, Barnouin OS, Robinson MS, Denevi BW, Blewett DT, Head JW, Izenberg NR, Solomon SC, Head JW (2010) Exposure of spectrally distinct material by impact craters on Mercury: implications for global stratigraphy. *Icarus* 209:210–223
- Espósito LW (1984) Sulfur dioxide - Episodic injection shows evidence for active Venus volcanism. *Science* 223:1072–1074. (ISSN 0036-8075) doi:[10.1126/science.223.4640.1072](https://doi.org/10.1126/science.223.4640.1072)
- Espósito LW, Copley M, Eckert MR, Gates L, Stewart AIF, Worden H (1988) Sulfur dioxide at the Venus cloud tops, 1978–1988. *J Geophys Res* 93:5267–5276
- Ford PG, Pettengill GH (1992) Venus topography and kilometer-scale slopes. *J Geophys Res* 97:13103–13114
- Garate-Lopez I, Hueso R, Sánchez-Lavega A, Peralta J, Piccioni G, Drossart P (2013) A chaotic long-lived vortex at the southern pole of Venus. *Nat Geosci* 6:254–257. doi:[10.1038/ngeo1764](https://doi.org/10.1038/ngeo1764)
- Gérard J-C, Cox C, Saglam A, Bertaux J-L, Villard E, Nehmé C (2008) Limb observations of the ultraviolet nitric oxide nightglow with SPICAV on board Venus Express. *J Geophys Res Planet* 113(E5). doi:[10.1029/2008JE003078](https://doi.org/10.1029/2008JE003078)
- Goudge TA, Head JW, Kerber L, Blewett DT, Denevi BW, Domingue DL, Gillis-Davis JJ, Gwinner K, Helbert J, Holsclaw GM, Izenberg NR, Klima RL, McClintock WE, Murchie SL, Neumann GA, Smith DE, Strom RG, Xiao Z, Zuber MT, Solomon SC (2014) Global inventory and characterization of pyroclastic deposits on Mercury: new insights into pyroclastic activity from MESSENGER orbital data. *J Geophys Res* doi:[10.1002/2013JE004480](https://doi.org/10.1002/2013JE004480) (Article first published online: 28 MAR 2014)
- Hawkins III SE et al (2007) The Mercury dual imaging system on the MESSENGER spacecraft. *Space Sci Rev* 131:247–338
- Kerber L, Head JW, Solomon SC, Murchie SL, Blewett DT, Wilson L (2009) Explosive volcanic eruptions on Mercury: Eruption conditions, magma volatile content, and implications for interior volatile abundances. *Earth Planet Sci Lett* 285(3–4):263–271. doi:[10.1016/j.epsl.2009.04.037](https://doi.org/10.1016/j.epsl.2009.04.037)
- Kerber L, Head JW, Blewett DT, Solomon SC, Wilson L, Murchie S, Robinson MS, Denevi BW, Domingue DL (2011) The global distribution of pyroclastic deposits on Mercury: the view from MESSENGER flybys 1–3. *Planet Space Sci* 59:1895–1909
- Killen R, Cremonese G, Lammer H et al (2007) Processes that promote and deplete the exosphere of Mercury. *Space Sci Rev* 132(2–4):433–509. doi:[10.1007/s11214-007-9232-0](https://doi.org/10.1007/s11214-007-9232-0)
- Khatuntsev IV, Patsaeva MV, Titov DV, Ignatiev NI, Turin AV, Limaye SS, Markiewicz WJ, Almeida M, Roatsch TH, Moissl R (2013) Cloud level winds from the Venus Express Monitoring Camera imaging. *Icarus* 226(1):140–158. <http://dx.doi.org/10.1016/j.icarus.2013.05.018>
- Kouyama T, Imamura T, Nakamura M, Satoh T, Futaana Y (2013) Long-term variation in the cloud-tracked zonal velocities at the cloud top of Venus deduced from Venus Express VMC images. *J Geophys Res Planet* 118:37–46. doi: [10.1029/2011JE004013](https://doi.org/10.1029/2011JE004013)
- Lawrence DJ, Feldman WC, Goldsten JO, Maurice S, Peplowski PN, Anderson BJ, Bazell D, McNutt RL, Nittler LR, Prettyman TH, Rodgers DJ, Solomon SC, Weider SZ (2013) Evidence for water ice near Mercury's North pole from MESSENGER neutron spectrometer measurements. *Science* 292–296 (Published online 29 November 2012)
- Leverington DW (2004) Volcanic rilles, streamlined islands, and the origin of outflow channels on Mars. *J Geophys Res* 109:E10011. doi:[10.1029/2004JE002311](https://doi.org/10.1029/2004JE002311)
- Limaye SS (2007) Venus atmospheric circulation: known and unknown. *J Geophys Res* 112: E04S09. doi:[10.1029/2006JE002814](https://doi.org/10.1029/2006JE002814)

- Limaye SS, Suomi VE (1981) Cloud motions on Venus: global structure and organization. *J Atmos Sci* 38:1220–1235
- Limaye SS, Kossin JP, Rozoff C, Piccioni G, Titov DV, Markiewicz WJ (2009) Vortex circulation on Venus: dynamical similarities with terrestrial hurricanes. *Geophys Res Lett* 36(4):L04204. doi:[10.1029/2008GL036093](https://doi.org/10.1029/2008GL036093)
- Linkin VM, Blamont J, Lipatov A, Devyatkin SI, D'yachkov AV, Ignatova BI, Kerzhanovich VV, Malique C, Stadnyk VI et al (1986) Vertical thermal structure of the Venus atmosphere from temperature and pressure measurements. *Pisma V Astron* 12(2):100–105
- Lucey PG (2013) A wet and volatile Mercury. *Science* 282–283. doi:[10.1126/science.1232556](https://doi.org/10.1126/science.1232556)
- Luz D et al (2011) Venus's southern polar vortex reveals precessing circulation. *Science* 332:577–580
- Mahieux et al (2012) *J Geophys Res Planet* 117:E07001. doi:[10.1029/2012JE004058](https://doi.org/10.1029/2012JE004058)
- Margot JL, Peale SJ, Jurgens RF, Slade MA, Holin IV (2007) Large longitude libration of Mercury reveals a molten core. *Science* 316:710–714
- Marcq E, Bertaux J-L, Montmessin F, Belyaev D (2013) Variations of sulphur dioxide at the cloud top of Venus's dynamic atmosphere. *Nat Geosci* 6:25–28. doi:[10.1038/ngeo1650](https://doi.org/10.1038/ngeo1650)
- Migliorini A, Altieri F, Zasova L, Piccioni G, Bellucci G, Cardesin Moineau A, Drossart P, D'Aversa E, Carrozzo FG, Gondet B, Bibring J-P (2011) Oxygen airglow emission on Venus and Mars as seen by VIRTIS/VEX and OMEGA/MEX imaging spectrometers. *Planet Space Sci* 59:981–987
- Montmessin F, Bertaux J-L, Lefèvre F, Marcq E, Belyaev D, Gérard J-C, Korabiev O, Fedorova A, Sarago V, Vandaele AC (2011) A layer of ozone detected in the nightside upper atmosphere of Venus. *Icarus* 216(1):82–85. <http://dx.doi.org/10.1016/j.icarus.2011.08.010>
- Mueller N, Helbert J, Erard S, Piccioni G, Drossart P (2012) Rotation period of Venus estimated from Venus Express VIRTIS images and Magellan altimetry. *Icarus* 217(21):474–483
- Murray BC, Strom RG, Trask NJ, Gault DE (1975) Surface history of Mercury: implications for terrestrial planets. *J Geophys Res* 80:2508–2514
- Nittler LR, Weider SZ, Starr RD, Chabot N, Denevi BW, Ernst CM, Goudge TA, Head JW, Helbert J, Klima RL, McCoy TJ, Solomon SC (2014), Sulfur-depleted composition of Mercury's largest pyroclastic deposit: implications for explosive volcanism and surface reflectance on the innermost planet. Presented at the 45th Lunar and planetary science conference, held 17–21 March, 2014 at The Woodlands, Texas. LPI Contribution No. 1777, p 1391
- Oberbeck VR, Quaide WL, Arvidson RE, Aggarwal HR (1977) Comparative studies of lunar, Martian and Mercurian craters and plains. *J Geophys Res* 82. doi:[10.1029/JB082i011p01681](https://doi.org/10.1029/JB082i011p01681)
- Paige, DA et al (2013) Thermal stability of volatiles in the north polar region of Mercury. *Science* 339:300–303. doi:[10.1126/science.1231106](https://doi.org/10.1126/science.1231106)
- Piccialli AS, Tellmann DV, Titov SS, Limaye IV, Khatuntsev M, Pätzold B, Häusler Titov DV (2012) Dynamical properties of the Venus mesosphere from the radio-occultation experiment VeRa onboard Venus Express. *Icarus* 217(2):669–681. <http://dx.doi.org/10.1016/j.icarus.2011.07.016> (Advances in Venus Science)
- Robinson MS, Lucey PG (1997) Recalibrated Mariner 10 color mosaics: implications for mercurian volcanism. *Science* 275:197–200
- Schubert G (1983) General circulation and the dynamical state of the Venus atmosphere. In: Venus, Hunten D et al (eds) University of Arizona Press, vol 1143, p 1983
- Schubert G (2010) Venus rotation, Paper presented at the VEXAG. In: International Venus Workshop, 2010. venus.wisc.edu/venus-workshop-submission/files/schubert_gerald-2.pdf
- Seiff A (1987) Further information on structure of the atmosphere of Venus derived from VeGa balloon and lander mission. *Adv Space Res* 7(12):323–328. doi:[10.1016/0273-1177\(87\)90239-0](https://doi.org/10.1016/0273-1177(87)90239-0)
- Shalygin EV, Markiewicz WJ, Basilevsky AT, Titov DV, Ignatiev NI, Head JW Bright transient spots in ganiki chasma, Venus. Presented at the 45th Lunar and planetary science conference, held 17–21 March, 2014 at The Woodlands, Texas. LPI Contribution No. 1777, p 2556
- Slade MA, Butler BJ, Muhleman DO (1992) Mercury radar imaging: evidence for polar ice. *Science* 258:635–640

- Smith DE, Zuber MT, Phillips RJ, Solomon SC, Hauck II SA, Lemoine FG, Mazarico E, Neumann GA, Peale SJ, Margot J-L, Johnson CL, Torrence MH, Perry ME, Rowlands DD, Goossens S, Head JW, Taylor AH (2012) Gravity field and internal structure of Mercury from MESSENGER. *Science* 336(6078):214–217. doi:[10.1126/science.1218809](https://doi.org/10.1126/science.1218809)
- Smrekar SE, Stofan ER, Mueller N, Treiman A, Elkins-Tanton AL, Helbert J, Piccioni G, Drossart P (2010) Recent hotspot volcanism on Venus from VIRTIS emissivity data. *Science* 328:605–608
- Solomon SC (2003) Mercury: the enigmatic innermost planet. *Earth Planet Sci Lett* 216:441–455
- Soret L, J-C Gérard, Piccioni G, Drossart P (2014) Time variations of O₂(a¹Δ) nightglow spots on the Venus nightside and dynamics of the upper mesosphere. *Icarus* 237:306–314. doi:[10.1016/j.icarus.2014.03.034](https://doi.org/10.1016/j.icarus.2014.03.034)
- Staley D (1970) The adiabatic lapse rate in the Venus atmosphere. *J Atmos Sci* 27:219–223
- Strom RG, Trask JJ, Guest JE (1975) Tectonism and volcanism on Mercury. *J Geophys Res* 80:2478–2507
- Suomi VE, Limaye SS (1978) Further evidence of vortex circulation on Venus. *Science* 201:1009–1011
- Svedhem H, Titov D, Taylor F, Witasse O (2009) Venus Express mission. *J Geophys Res* 114: E00B33. doi:[10.1029/2008JE003290](https://doi.org/10.1029/2008JE003290)
- Taylor FW (2006) Venus before Venus express. *Planet Space Sci* 2006:1249–1262
- Taylor FW, Beer R, Chahine MT, Diner DJ, Elson LS, Haskins RD, McCleese DJ, Martonchik JV, Reichley PE, Bradley SP, Delderfield J, Schofield JT, Farmer CB, Froidevaux L, Leung J, Coffey MT, Gille JC (1980) Structure and meteorology of the middle atmosphere of Venus. Infrared remote sensing from the Pioneer orbiter. *J Geophys Res* 85:7963–8006. <http://dx.doi.org/10.1029/JA085iA13p07963>
- Vasavada AR, Paige DA, Wood SE (1999) Near-surface temperatures on mercury and the moon and the stability of polar ice deposits. *Icarus* 141(1999):179–193
- Watson KB, Murray BC, Brown H (1961) The behavior of volatiles on the Lunar surface. *J Geophys Res* 66(9):3033–3045
- Watters TR, Robinson MS, Beyer RA, Banks ME, Bell III JF, Pritchard ME, Hiesinger H, van der Bogert CH, Thomas PC, Turtle EP, Williams NR (2010) Evidence of recent thrust faulting on the moon revealed by the Lunar Reconnaissance Orbiter Camera. *Science* 329(5994):936–940. doi:[10.1126/science.1189590](https://doi.org/10.1126/science.1189590)
- Watters TR, Solomon SC, Klimczak C, Freed AM, Head JW, Ernst CM, Blair DM, Goudge RA, Byrne PK (2012) Extension and contraction within volcanically buried impact craters and basin on Mercury. *Geology* 40:1123–1126. doi:[10.1130/G33725.1](https://doi.org/10.1130/G33725.1)
- Wetherill G (1994) Provenance of the terrestrial planets. *Geochim Comochim Acta* 58:4513–4520
- Wilhelms DE (1976) Mercurian volcanism questioned. *Icarus* 28:551–558

Inner Solar System

Prospective Energy and Material Resources

Badescu, V.; Zacny, K. (Eds.)

2015, XXVII, 504 p. 212 illus., 158 illus. in color.,

Hardcover

ISBN: 978-3-319-19568-1